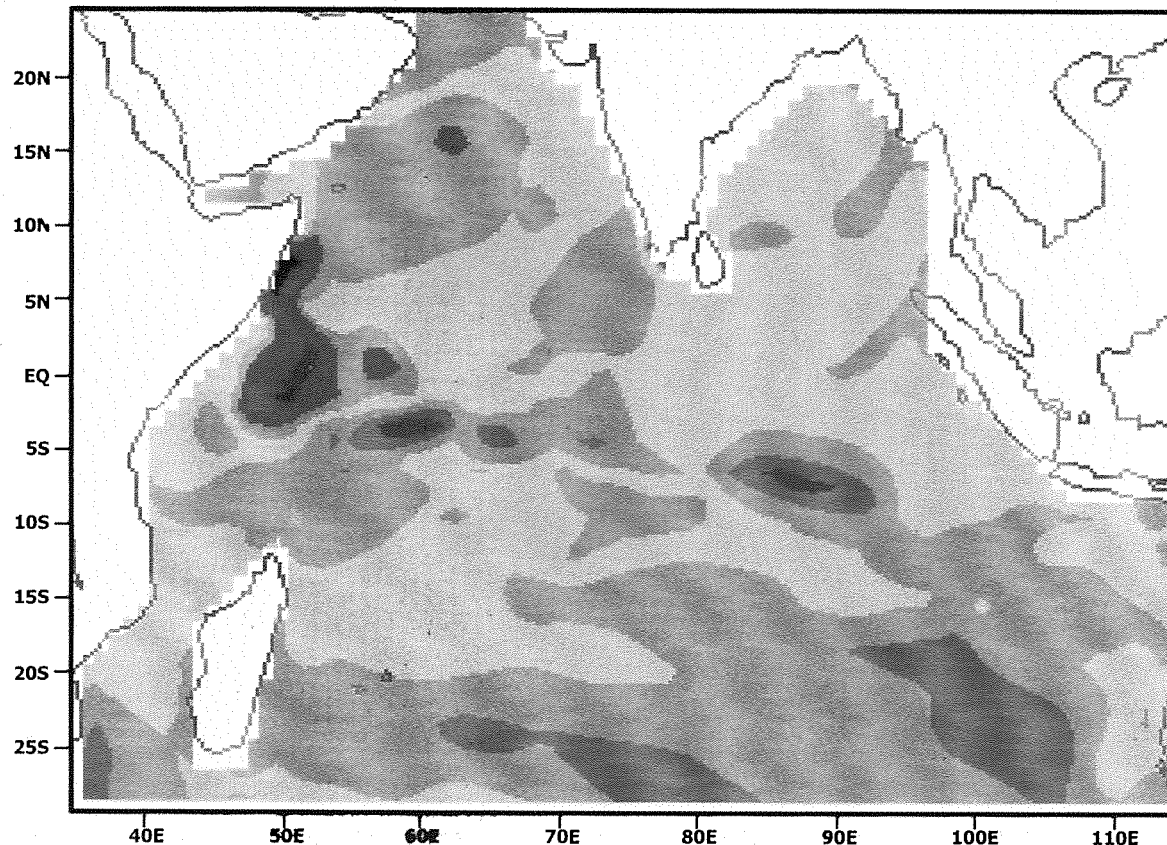


Behaviour of North Indian Ocean During the Onset Phases of Southwest Monsoon Using Satellite Winds



December 2000



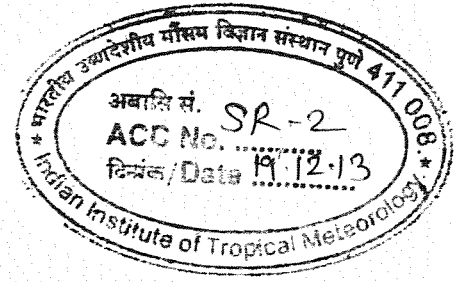
Indian Institute Of Tropical Meteorology,

Dr. Homi Bhabha Road, Pashan,

Pune - 411 008

SR-2

IITM - SAC
(IRS-P4 MSMR Application)
Collaborative Project
Research Report



**Behaviour of North Indian Ocean
During the Onset Phases of Southwest
Monsoon Using Satellite Winds**

**P.S.Salvekar, S.K.Behera, D.W.Ganer,
A.A.Deo and P.Rahul Reddy**

Indian Institute of Tropical Meteorology, Pune - 411 008

and

Sujit Basu and Raj Kumar

Space Applications Center, Ahmedabad - 380 015

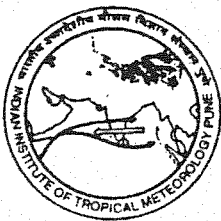
December 2000



Indian Institute Of Tropical Meteorology,
Dr.Homi Bhabha Road, Pashan,
Pune - 411 008

C o n t e n t s

	Page No.
Foreword	
Preface	
Abstract	1
1. Introduction	2
2. Model	4
3. Numerical Procedure	6
4. Results & Discussion	7
4.1 SST and Circulation Fields in the Upper and Lower Layer	8
4.2 Latitude/Longitude – Time Cross Sections	10
4.3 Variability in the Individual Regions	13
5. Conclusions	14
Acknowledgments	
References	
List Of Figures	



भारतीय उष्णदेशीय मौसम विज्ञान संस्थान INDIAN INSTITUTE OF TROPICAL METEOROLOGY

(विज्ञान और प्रौद्योगिकी मंत्रालय का एक स्वायत्त संस्थान, भारत सरकार के अधीन)
(An Autonomous Institute of the Ministry of Science and Technology, Govt. of India)

G.B.Pant
DIRECTOR

Tel: (020)5893600
Fax: (020)5893825

FOREWORD

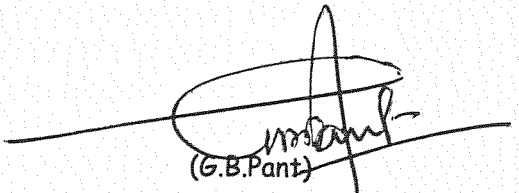
The annual cycle of the monsoon winds induces dramatic changes in the thermodynamic characteristics of the upper north Indian Ocean. The reversal of monsoon winds, the equatorial wave guide and the northern boundaries provide ample mechanisms for the variability in hydrodynamic fields. Ocean models provide a reasonable scope for understanding and predicting the fields like SST & currents and their variabilities in both space and time. Uncertainties in estimations of these fields and inadequate sampling coverages are some of the reasons that have made model simulation studies so attractive in recent years. Model studies in the Pacific Ocean, suggest a dominating influence of surface winds in determining upper layer thermodynamic structure. The interannual SST variability in equatorial Pacific Ocean is dominantly influenced by the changes in trade winds. However, Pacific Ocean does not experience the large scale seasonal reversal of surface winds and large variability in surface heat flux every year, like monsoon conditions in Indian Ocean.

The ocean modelling activity was started in the Indian Institute of Tropical Meteorology about a decade ago and now the ocean modelling group of the Theoretical Studies Division has acquired a prominent position among the groups in country for North Indian Ocean Modelling studies. The joint collaborative project between Indian Institute of tropical Meteorology, Pune and Space Applications Centre, Ahmedabad for studying North Indian Ocean Circulation using Satellite data is an example of the successful use of satellite data in weather and climate research. Last year India has launched Oceansat -1 the first Indian Satellite dedicated for oceanic studies. Main aim of the collaborative project is the application of MSMR winds in the thermodynamic ocean model for simulation and prediction of SST, currents and mixed layer depth over North Indian Ocean. As a first step, SSM/I winds that are similar to MSMR winds and NCEP heat fluxes are used as input to the thermodynamic model and numerical experiments are carried out in producing SST and currents in the North Indian Ocean

during the onset phases of SW monsoon, in response to inter-annually varying daily SSM/I surface winds for the period 1994 to 1996. From this numerical experiment, first time it is noticed in the computed SST fields that minimum SST gradient of $3^{\circ}\text{C}/2000\text{ km}$ is observed due north and due west direction from the region 2°S - 7°S , 60°E - 65°E ; about 8 to 10 days prior to the arrival of SW monsoon near Kerala coast. Further, it is also found that the model works with reasonably good accuracy by considering the input in the daily scale.

The model can be further tested with the MSMR data. The contents of this report will be useful to the scientists engaged in research on atmospheric and oceanic studies, monsoon studies as well as air-sea interaction studies. I am very happy to see that the project partners are bringing out a joint report which I am sure will be a useful document for users and scientists alike.

Pune
December, 2000



(G.B. Pant)

भारत सरकार
अन्तरिक्ष विभाग
अन्तरिक्ष उपयोग केन्द्र
सैक डाक घर, अहमदाबाद - 380 053. (भारत)
दूरभाष : 6761188, 6740256
फैक्स : 079-6765410, 6767708



GOVERNMENT OF INDIA
DEPARTMENT OF SPACE
SPACE APPLICATIONS CENTRE
SAC.P.O., AHMEDABAD- 380 053. (INDIA)
PHONE : 6761188, 6740256
FAX : 079-6765410, 6767708

A.K.S. GOPALAN
DIRECTOR

TEL : 6764956
FAX: 6768073

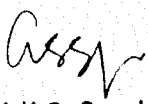
PREFACE

Recently India has launched Oceansat-1, the first Indian satellite dedicated to oceanic applications. This satellite carries onboard a multichannel scanning microwave radiometer (MSMR) providing frequent wind observations and these winds are being used on an experimental basis in an assimilation system in the National Centre for Medium Range Weather Forecast for generating six hourly analysed MSMR wind vectors which are being used by different organisations for a variety of applications. There is a joint collaborative project between the Indian Institute of Tropical Meteorology and Space Applications Centre for studying the Indian Ocean circulation behaviour using a thermodynamic Indian Ocean model which is known to simulate the interannual variability of the north Indian Ocean circulation and sea surface temperature quite successfully. It is expected that the model will be useful for the purpose of predicting oceanic dynamic and thermodynamic characteristics like currents, SST etc. after more testing and fine-tuning and with proper forcing data.

As a prelude to utilisation of actual MSMR winds, an effort has been made by the scientists of both the organisations to study the behavior of the North Indian Ocean during the onset phases of the southwest monsoon for the years 1994 to 1996 using the model mentioned and daily analysed SSMI winds (which are analogous to analysed MSMR winds) and NCEP heat fluxes. Considerable amount of research effort has gone into this report to determine the behaviour of ocean parameters during southwest monsoon onset phase. The study has led to interesting observations of thermal gradient during the onset phases of southwest monsoon. Model SST has been found to be in close agreement with NCEP analysed SST as a result of forcing by daily winds and fluxes.

I hope that more fruitful collaborations will emerge as a result of this ongoing joint collaborative effort between the two institutes and I also hope that the ocean modeling community in general and Indian Ocean modeling community in particular will immensely benefit from the outcome of this joint effort.

Ahmedabad
December 13, 2000


(A.K.S. Gopalan)

Abstract

Interannual variability of the North Indian Ocean circulation and SST were simulated successfully by Behera et.al(1998,1999) using a 2½ layer thermodynamic numerical ocean model. In the present study the same model is used to simulate the SST and the currents during the onset phases of the three years from 1994 to 1996 using daily SSM/I winds and NCEP heat fluxes. The results are presented and discussed for 30 days period from 16th May to 13th June to determine the behaviour of ocean parameters during SW monsoon onset phase. The maximum variability in the simulated SST is found along Somali coast, Indian coasts and equatorial regions. The maximum and minimum SST in the Arabian Sea and west equatorial region is found to be $> 30^{\circ}\text{C}$ and 25°C during the onset phases of all the three years and they are in agreement with Reynolds SST. Upper and lower layer circulation fields do not show prominent interannual variability but SST gradients in the north - south as well as east - west directions in the west of 80°E are found to change significantly. It can be inferred from the computed SST fields that minimum SST gradient of $3^{\circ}\text{C}/2000\text{ km}$ is observed due north and due west direction from the region $2^{\circ}\text{S}-7^{\circ}\text{S}$, $60^{\circ}\text{E}-65^{\circ}\text{E}$; about 8 to 10 days prior to the arrival of SW monsoon near Kerala coast.

1. Introduction

The annual cycle of the monsoon winds induces dramatic changes in the thermodynamic characteristics of the upper north Indian Ocean. The reversal of monsoon winds, the equatorial wave guide and the northern boundaries provide ample mechanisms for the variability in hydrodynamic fields. The local strong southwesterly winds during summer monsoon help in cooling the sea surface by evaporation and upwelling. These local changes in turn excite propagating signals that travel large distances to remotely influence far away regions. For example, these signals that are carried by equatorial Kelvin waves influence the Bay of Bengal circulation. The seasonal variability in the thermodynamic characteristics of the region is understood to some extent but their interannual variabilities have come to light only in this decade.

Ocean models provide a reasonable scope for understanding and predicting the fields like SST & currents and their variabilities in both space and time. Uncertainties in estimations of these fields and inadequate sampling coverages are some of the reasons that have made model simulation studies so attractive in recent years. Evolution of ocean circulation and heat content in the upper layers generally depend more on the surface forcing fields than on the internal dynamics. Hence, reliable knowledge of the forcings in both space and time is essential for the modelling studies. However, uncertainties still remain in estimating the fluxes, may be due to the sampling problems both in space and time and due to

uncertainties in prescribing the drag coefficients, which lead to large discrepancies in different analyses of the fluxes. To avoid sampling problems, climatological fluxes of all the available historical observations for each calendar month, are generally used in modelling studies. Therefore, Hellerman and Rosenstein (1983) produced climatological monthly mean wind stress fields over the world ocean, are widely used in ocean modelling studies. Monthly fields of interannual wind stress are also available over some part of the world ocean, e.g. the FSU pseudo-stress fields. However, heat and freshwater flux estimation on any time scale have serious sampling and computational problems. Hence, most of the modelling studies of tropical oceans have been preceded with the observed anomalies only in the momentum flux. Besides their use in the studies of ocean physics and dynamics, ocean models are being coupled with atmospheric models. Atmospheric models also produce momentum fluxes that are more realistic than the other two fluxes .

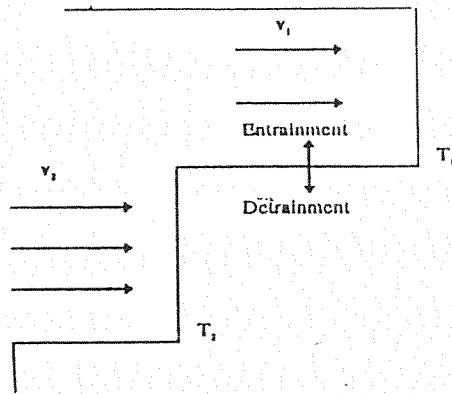
Since the wind stress is one of the major components of surface forcings in the ocean models, it is crucial to understand model sensitivity to the wind stress forcings. Luther and O'Brien (1989) simulated the interannual variability in the upper layer circulation of the Indian Ocean by forcing a simple reduced gravity model with interannual Cadet and Diehl (1984) wind fields. Although reduced gravity model can not provide many other observed fields, the importance of such simple models can not be ignored due to their simplicity in understanding and interpreting

the results. Model studies in the Pacific Ocean, suggest a dominating influence of surface winds in determining upper layer thermodynamic structure. The interannual SST variability in equatorial Pacific Ocean is dominantly influenced by the changes in trade winds. However, Pacific Ocean does not experience the large scale seasonal reversal of surface winds and large variability in surface heat flux every year, like monsoon conditions in Indian Ocean. Behera et.al (1998) used the model of intermediate complexity (McCreary et.al. ; 1993, hereafter referred to as MKM), to simulate the upper layer circulation along the east coast of India. Same model is also used by Behera et.al.(1999) to examine the contribution of interannually varying surface winds on the SST variability of the Indian Ocean. Further, the dipole structure that was observed in the tropical Indian Ocean during 1994 around 10^0 S, was very well simulated by Salvekar et.al (2000). In the present study the same model (MKM) is used in producing SST and currents in the north Indian Ocean during the onset phases of SW monsoon in response to inter-annually varying daily SSM/I surface winds for the period 1994 to 1996.

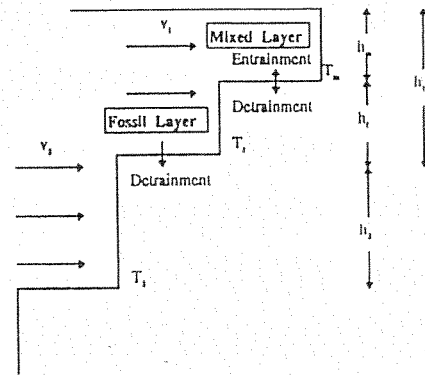
2. The Model

The $2\frac{1}{2}$ layer thermodynamic ocean model used in this study, is fully described in MKM. In short, the model ocean consists of two active layers overlying a deep motionless layer of infinite depth. The upper two active layers interact with each other through entrainment and detrainment while conserving mass and

heat of the total system. In simpler form the surface uppermost layer is a single layer with a thickness of h_1 and temperature T_1 . However, once entrainment and detrainment start taking place the surface layer assumes a more complex form in which it separates into two sub-layers i.e. a well-mixed upper turbulent layer of thickness h_m and temperature T_m and a non-turbulent fossil layer of thickness h_f and temperature T_f . In both the cases i.e. in the simple one layer form and the complex sub-layer form, the surface layer has velocity v_1 . Thus, there is no vertical shear in the velocity field in the sub-layers of the surface layer as shown below.



**Model layer Structure in
the Simple Form With
Single Upper layer**



**The Complex form in which
Upper Layer is divided into
Mixed Sub-Layer and Fossil**

The uppermost sub-layer of the surface layer that can be termed as upper mixed layer entrains or detrains water in a process in which the mixing is maintained by turbulence generated

by both wind stirring and cooling at the surface. The non-turbulent fossil layer i.e. the lower sub-layer of the surface layer being formed by the detrainment of water from the upper mixed layer, is kept isolated from the surface turbulence. However, it can be engulfed into the mixed layer either during the strong entrainment or upwelling regimes, when h_1 becomes shallow significantly. There is also provision for detrainment of water from the upper surface layer to the model second layer, to conserve mass of the layers, because of the fact that entrainment through the base of the surface layer takes mass from the second layer. The second layer has velocity v_2 , thickness h_2 and temperature T_2 . In this study, the initial values of $h_1 = 65$ m and $h_2 = 250$ m are considered. The temperature of the uppermost turbulent sub-layer is considered as representative of Sea Surface Temperature (SST).

3. Numerical Procedure

The model equations are solved numerically on staggered 'Arakawa C' grid over the horizontal domain 30S to 25N and 35E to 115E with a horizontal resolution of 55 km. The wind stress is derived from SSM/I winds, with drag coefficient $C_D = 1.5 \times 10^{-3}$ and air density $\rho = 1.175$ kg m⁻³. Linear interpolation is used to get the SSM/I wind input at model grid points, as well as to get data at model time step. Leap-frog scheme is used for time integration with a time step of one hour. Time filter is applied at every 41st time step to avoid time splitting instability. The surface heat flux used as a thermal forcing in the model is derived from the daily net solar

radiation (incoming - outgoing), air temperature, specific humidity and scalar wind magnitudes. These fields are derived from the daily NCEP data set for computation of sensible and latent heat fluxes, from these fields bulk formulae with the model predicted SST is used instead of observed climatological SST. The drag coefficient used for sensible heat flux is $C_s = 0.001$ and for latent heat flux is $C_L = 0.0015 + 0.0033 (T_m - T_a)$, for $|T_m - T_a| \leq 2^0 \text{ C}$, beyond which range, C_L has maximum value of 0.002 and minimum of 0.001. For simplicity, a linear variation of C_L with the variation of air-sea temperature is assumed (MKM).

4. Results and Discussion

Initially the model was spun up for 7 years with climatological winds obtained by 5 year average of five days mean SSM/I winds for the period 1992 to 1996 and climatological NCEP heat flux. The numerical solution reached a quasi-equilibrium state after 6th year. Therefore, the model solutions from 7th year are considered as model climatology for the inter-annual runs. Subsequently, the model equations were integrated for further 3 years with inter-annually varying daily SSM/I wind and daily NCEP heat flux, from 1 Jan 1994 to 31 Dec 1996.

The model results over the domain $10^0 \text{ S} - 25^0 \text{ N}$, $40^0 \text{ E} - 100^0 \text{ E}$, during the onset phases of SW monsoon for all the three years, are shown at the interval of two days, for the period 16th May to 13th June (Fig-15). Since the actual onset date varies from

28th May to 8th June in these three years, the period 16th May to 13th June was considered in order to have sufficient time period for analysing SST and currents before and after the actual onset date. In the year 1994, the onset of SW monsoon over Kerala coast, was on 28th May. In the year 1995 it was on 8th June and in the year 1996 it was declared on 3rd June.

4.1 SST and Circulation fields in the Upper and Lower layer

Results for the depth averaged currents and temperature fields for the year 1994 are shown in Figure 1 to Figure 5, for the upper and lower layer, in the left and right panels. As already discussed in the section 2, the depth averaged temperature for the upper layer is denoted as SST. The maximum SST of 30° C is found in the northern Arabian Sea around 15° N-18° N, 65° E-70° E and the minimum SST of about 25° C is found near Somali coast around EQ-3° S, 45° E-50° E which persist beyond the onset date. However, the SST gradient between the regions 60° E-65° E, 2° S-7° S (hereafter denoted as region A), 13° N-18° N, 65° E-70° E (region B) and EQ-5° S, 45° E-50° E (region C) are found to change significantly from year to year near the onset date. During 1994, maximum SST difference between the region A & C is about 3° C, which reduces to 1.5° C from 28th May. SST difference between A & B is greater than 3° C, which persists till 1st June and it almost disappeared from 5th June, which clearly indicates surface cooling. Surface currents show increasing trend from 26th

May. North-south temperature difference between the head Bay and east equatorial Indian Ocean is about 1.5° C throughout the period. Lower layer circulation and SST pattern east of 80° E (Bay of Bengal and equatorial Indian Ocean) remains almost same throughout the period.

During 1995, (fig 6 to 10) from 16th May, maximum SST in north Arabian Sea did not enhance beyond 29.5° C. Warm Somali coast and relatively cool Arabian Sea resulted into very weak SST gradient both in the north south and east west direction, till 80° E i.e. between the region A & B as well as between A & C. The gradient between 6° S to 20° N starts building after 26th May. The gradient is greater than 2.5° C from 30th May. In general SSTs in the west of 80° E are found weak during 1995, which resulted into late onset. SSTs in the Bay of Bengal and east equatorial region do not show significant change. Lower level equatorial Indian Ocean is found to be warm during 1995. Results shown in figs. 11-15, are for 1996, during which SST pattern for the whole region in the west of 80° E is found to be similar to that of year 1994. Abnormal surface cooling is seen in the southeast of Sri Lanka (68° E- 78° E, 2° N - 8° N) throughout the period. This region of cooling is enhanced after 1st June. The cooling is found to be penetrated in the lower layer from 3rd June as seen from the corresponding lower layer temperature field.

Before one week of the onset, the model currents are southeastward south of the equator up to 10° S and slowly become

northeastward in the region 3° S-EQ, 40° E- 75° E from the onset date. The northward currents become stronger near Somali coast. Strong southward currents from 3rd June are found from 6° S to 12° N. An anticyclonic gyre is well simulated near the coast in the region 6° S - EQ and the lowest SST of 25.5° C is found in the same region. This cooling may be due to the upwelling near the coast.

Lower layer circulation in all the three years shows 50% reduction in the magnitude of the currents as the lower layer circulation is dominantly influenced by Ekman pumping and radiation of waves from the equatorial region, whereas the strong surface wind forcings influence the upper layer circulation. The direction of the lower layer currents is opposite to that of the upper layer currents. During the onset phase, for all the years, the northward currents are found along west coast of India. The stronger surface northward currents near the Somali coast penetrate into the lower layer. The lower layer circulation pattern during the onset of 1995 and 1996 is more or less similar to the 1994 pattern.

4.2 Latitude / Longitude – Time cross sections

From the results discussed in the earlier section, it is seen that the region 'A' plays significant role before the onset date. Hence it seems that the region surrounding 'A' needs to be analysed in detail. The spatio-temporal advection of SST in the Arabian Sea is further analysed by considering latitude-time and

longitude- time cross section of SST anomalies for the 3 years, 1994, 1995 and 1996 from their mean. Fig.16 shows the latitude-time cross section (y-t plot) of SST anomalies from 20th April to 12th June and from 15° S to 15° N, for the three years 1994, 1995 and 1996, along the longitudes 55°E and 65°E. In 1994, at 55°E, the warm SST anomalies of the order of 0.3°C are found from 10°S to 5° S throughout the time, which supports the dipole event during the year 1994 (Behera et.al, 1999 a, ; Saji et.al , 1999).

It is seen that for the year 1994, negative anomalies of the order of 1.2° C appear in the belt of 5° S – EQ, at 55° E before 4 to 6 weeks of the onset and starts propagating northward slowly till the onset date. Speed of propagation is about 0.5 km/hr. For the year 1995 the negative SST anomalies, which were present in the year 1994, are replaced by positive SST anomalies of the order of 0.7° C, before 6 weeks of the onset and propagates slowly northward where as in the year 1996, these positive SST anomalies are found to be weak (~ 0.5° C) but still propagated towards north.

In 1994, near the onset date, negative SST anomalies occurred in the Arabian Sea between 5°N to 15°N, then they intensified up to 0.7° C and moved northward. In 1995, about 10 days before the onset, weak negative SST anomalies developed in the Arabian Sea between 5°N to 15°N and slowly propagated towards north, but in the year 1996, positive SST anomalies developed three weeks prior to the onset in the same region and

moved northward. These positive and negative anomalies near horn of Africa (10°N - 55°E) may be arising due to local wind stress effect.

Fig.17 Shows the longitude- time cross section (x-t plot) of SST anomalies from 20th April to 12th June and from 50°E to 80°E for the three years 1994, 1995 and 1996, along the latitudes 10°S , 5°S and Equator. It is seen that, along 10°S , in the belt of 50°E to 60°E , throughout the period, positive SST anomalies exist in 1994, and they are replaced by negative SST anomalies in the years 1995 and 1996, where as in the region of 60°E to 80°E , negative SST anomalies in 1994 are replaced by positive SST anomalies in the years 1995 and 1996. About 4 to 6 weeks before the onset, alternate bands of positive and negative SST anomalies occur along 5°S for the year 1994. 50°E to 60°E belt has negative SST anomalies (corresponding to negative anomalies in y-t plot along 55°E) while 60°E to 65°E belt has positive SST anomalies which prevail up to 15 days before the onset, then moved little westward and are stationary afterwards. 65°E to 75°E belt has negative SST anomalies, (corresponding to negative anomalies in y-t plot along 65°E) which persist up to a week after the onset date. The belt 75°E to 80°E has again positive anomalies which moved westward in the period considered. These are replaced by negative anomalies in the years 1995 and 1996. In 1995, along 5°S wide belt of negative SST anomalies exists from 55°E to 70°E , which is shifted westward to the belt of 50°E to 60°E , in 1996. In 1995 positive SST anomalies are present in the narrow belt of 70°E to

75° E, which strengthen and spread towards west in 1996. For all the years considered, it is observed that, at the time of onset, in the belt of 70° E to 75° E, negative SST anomalies are present. In 1994, along the equator, in the belt of 50° E to 60° E, negative SST anomalies ($\sim 0.5^{\circ}\text{C}$) are present which further decrease at the time of onset. In short, equatorial sea surface cools at the onset time. In 1995 and 1996 also, positive SST anomalies prevail, in the same belt along equator. In 1996 this anomalous warming is more ($\sim 0.9^{\circ}\text{C}$) near onset time than in 1995 viz. 0.5°C .

4.3 Variability in the individual regions

It is well known that the Arabian Sea is dynamically very active, hence the SST anomalies in the southwestern Arabian Sea are analysed in the regions 50°E - 60°E, 10° S - 2° S and 55° E - 65° E, EQ-5° N and the time series of the model SST anomalies for these two regions, for all the three years is shown in the fig. 18. During 1994, the warm SST anomalies for the region, 50°E - 60°E, 10°S - 2°S, are found before the onset and there is decrease in the amplitude of the SST anomalies after the onset, whereas in the region 55° E - 65° E, EQ-5° N, the maximum negative anomalies of 0.22°C are found for the same year. Such cooling is not seen in the remaining two years. The SST anomalies for the year 1995 and 1996 for the same regions are opposite to the year 1994. In the region 50° E - 60° E, 10° S - 2° S, the SST anomalies are negative in the year 1995 with maximum cooling a day before the onset, whereas very low positive SST anomalies are found in the year

1996 in the same region one week prior to the onset, which changes to the negative SST anomalies, after the onset. The warm SST anomalies in the region 55°E - 65°E , EQ - 5°N during both the years for 1995 and 1996 show the warming north of the equator in the Arabian Sea, which is in good agreement with the observed SST anomalies (Reynolds and Marsico, 1993).

5. Conclusions

From this numerical experiment, first time it is noticed that strong SST gradient, from region 'A' to region 'B' as well as from region 'A' to 'C', generally precede, at least 10 days prior to the onset date. The region 'A' (60°E - 65°E , 2°S - 7°S) plays significant role for considering north-south and east -west SST gradient. The circulation and SST field in the Bay of Bengal, do not show any significant interannual variability. Lower layer temperature field over east equatorial region is found to increase by 0.8°C to 1.2°C , for the year 1995.

It may be noted that even though the SSM/I observations from May to June are reduced drastically (as revealed from the climate diagnostic bulletins), the SSM/I surface wind analyses seems to be unaffected. This is because model SST and circulation patterns obtained from daily SSM/I wind and daily NCEP reanalysis winds are found to be comparable over the North Indian Ocean. From the encouraging results obtained in this experiment it

can be said that the model works with reasonably good accuracy by considering the input in the daily scale.

Acknowledgment : *The authors are thankful to the Director, IITM for his interest in the work and to the Director SAC for the research grant of this collaborative work. They are grateful to Dr. J.P. McCreary for kindly providing the ocean model. Thanks are due to Dr. Bryan Doty of COLA for kindly providing the GrADS software that was used in the preparation of the figures. Model integration of this work is carried out on the **Sun Ultra 60** workstation that is acquired under INDOMOD project for which authors are thankful to the DOD.*

References

Behera S K, Salvekar P S, Ganer D W and Deo A A, 1998: Interannual variability in simulated circulation along east coast of India, Indian. Jour. Mar. Sci., 27, 115-120.

Behera S K, Salvekar P S, Ganer D W, 1999 : Numerical investigation on wind induced interannual variability of north Indian Ocean SST, IITM Research Report No. RR-085.

Behera S K, Krishnanan R and Yamagata T, 1999 a : Unusual ocean atmosphere conditions in the tropical Indian Ocean during 1994, Geophysical Research Letters, 26, 19, 3001- 3004.

Cadet, D L and Diehl, B C, 1984: Interannual variability of surface fields over the Indian Ocean in recent decades, Mon. Wea. Rev., 112, 1921-1985.

Hellerman S and Rosenstein M , 1983 : Normal wind stress over the world ocean with error estimates; J. Phys. Oceanogr., 13, 1093-1104.

Luther, M E and O' Brien, J J, 1989, Modelling the variability in Somali Current, Meso-scale/ Synoptic coherent structure in Geophysical Turbulence; Eds J.C.J. Nihoul and B.M. Jamart, Elsevier Science Publ. 373-386.

McCreary J P, Kundu P K and Molinari R L, 1993: A numerical investigation of dynamics, thermodynamics, and mixed layer processes in the Indian Ocean; Prog. Ocean. 31, 181-244.

Reynolds R W and Marsico D C, 1993: An improved real-time global sea surface temperature analysis; J. Climate 6, 114-119.

Salvekar P S, Behera S K, Ganer D W, Deo A A, 2000: Role of SSM/I, NCEP and FSU surface winds in the evolution of dipole event during 1994 over Tropical Indian Ocean, Workshop on MSMR-First Results (Abstract).

Saji N H, Goswami B N, Vinay Chandran and Yamagata T, 1999: A Dipole in the tropical Indian Ocean, Nature, 401, 360 – 363.

List of Figures

Figure 1: *Model simulated Upper layer and Lower layer currents and SST for the dates 16, 18 and 20 May 1994.*

Figure 2: *Same as figure 1 except for the dates 22, 24 & 26 May 1994.*

Figure 3: *Same as figure 1 except for the dates 28, 30 May and 1 June 1994.*

Figure 4: *Same as figure 1 except for the dates 3, 5 and 7 June 1994.*

Figure 5: *Same as figure 1 except for the dates 9, 11 and 13 June 1994.*

Figure 6: *Model simulated upper layer and lower layer currents and SST for the 16,18 and 20 May 1995.*

Figure 7: *Same as figure 6 except for the dates 22, 24 and 26 May 1995.*

Figure 8: *Same as figure 6 except for the dates 28, 30 May and 1 June 1995.*

Figure 9: *Same as figure 6 except for the dates 3, 5 and 7 June 1995.*

Figure 10: *Same as figure 6 except for the dates 9, 11 and 13 June 1995.*

Figure 11: *Model simulated Upper layer and Lower layer currents and SST for the dates 16, 18 and 20 May 1996.*

Figure 12: *Same as figure 11 except for the dates 22, 24 and 26 May 1996.*

Figure 13 : *Same as figure 11 except for the dates 28, 30 May and 1 June 1996.*

Figure 14: *Same as figure 11 except for the dates 3, 5 and 7 June 1996.*

Figure 15: *Same as figure 11 except for the dates 9, 11 and 13 June 1996.*

Figure 16: *Latitude- time plot of model SST anomalies along 55 E and 65 E for the year 1994, 1995 and 1996.*

Figure 17: *Longitude - time plot of model SST anomalies along 10 S, 5 S and Equator, for the year 1994, 1995 and 1996.*

Figure 18: *Time series of model SST anomalies (3 days running mean)*

(a) *averaged over the region 50 E - 60 E, 10 S- 2 S for the period 19 May to June 1994.*

(b) *averaged over the region 55 E - 65 E, EQ - 5 N for the period 19 May to June 1994.*

(c) *averaged over the region 50 E - 60 E, 10 S- 2 S for the period 19 May to June 1995.*

(d) *averaged over the region 55 E - 65 E, EQ - 5 N for the period 19 May to June 1995.*

(e) *averaged over the region 50 E - 60 E, 10 S- 2 S for the period 19 May to June 1996.*

(f) *averaged over the region 55 E - 65 E, EQ - 5 N for the period 19 May to June 1996.*

Figure 1.

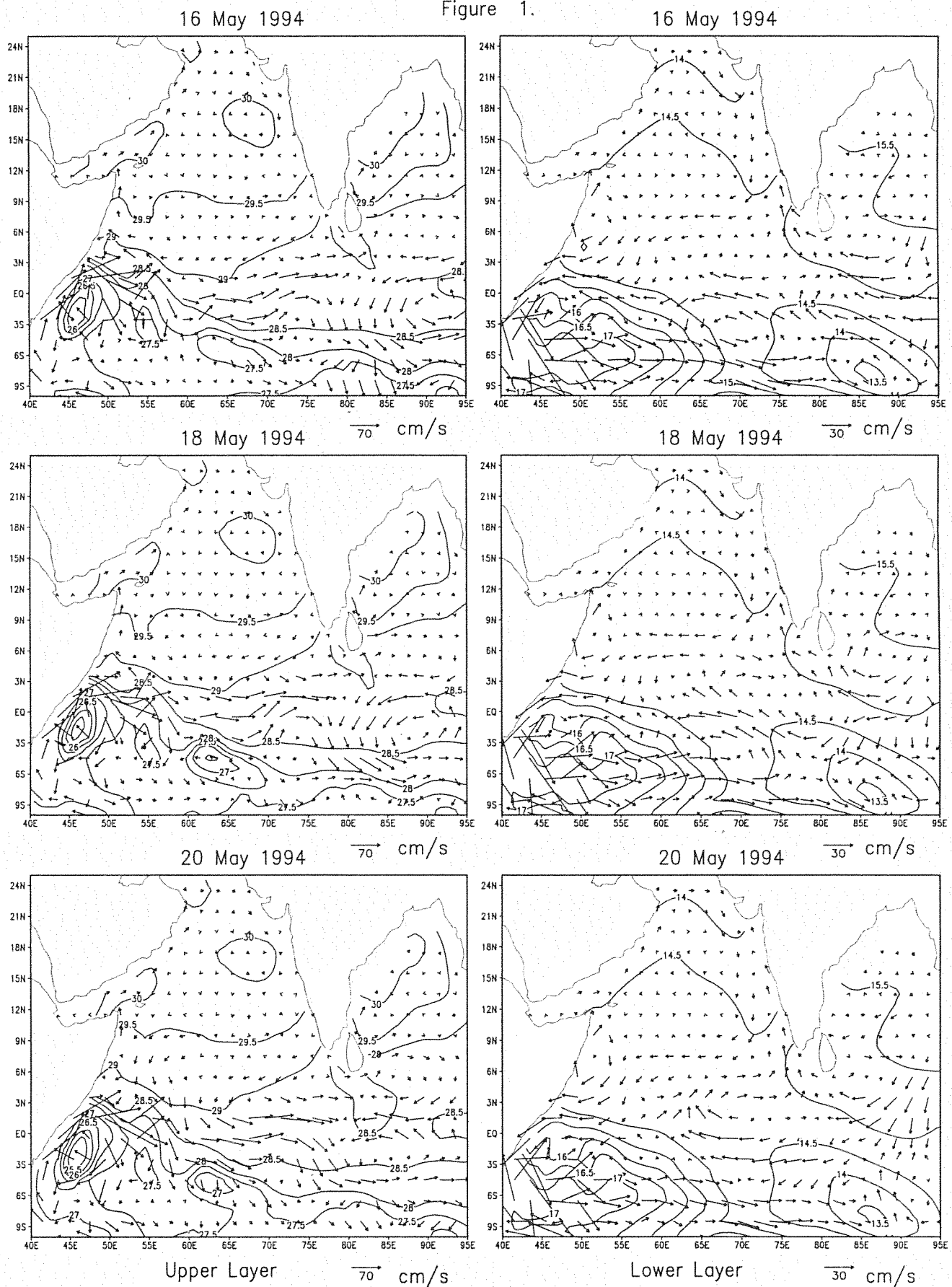
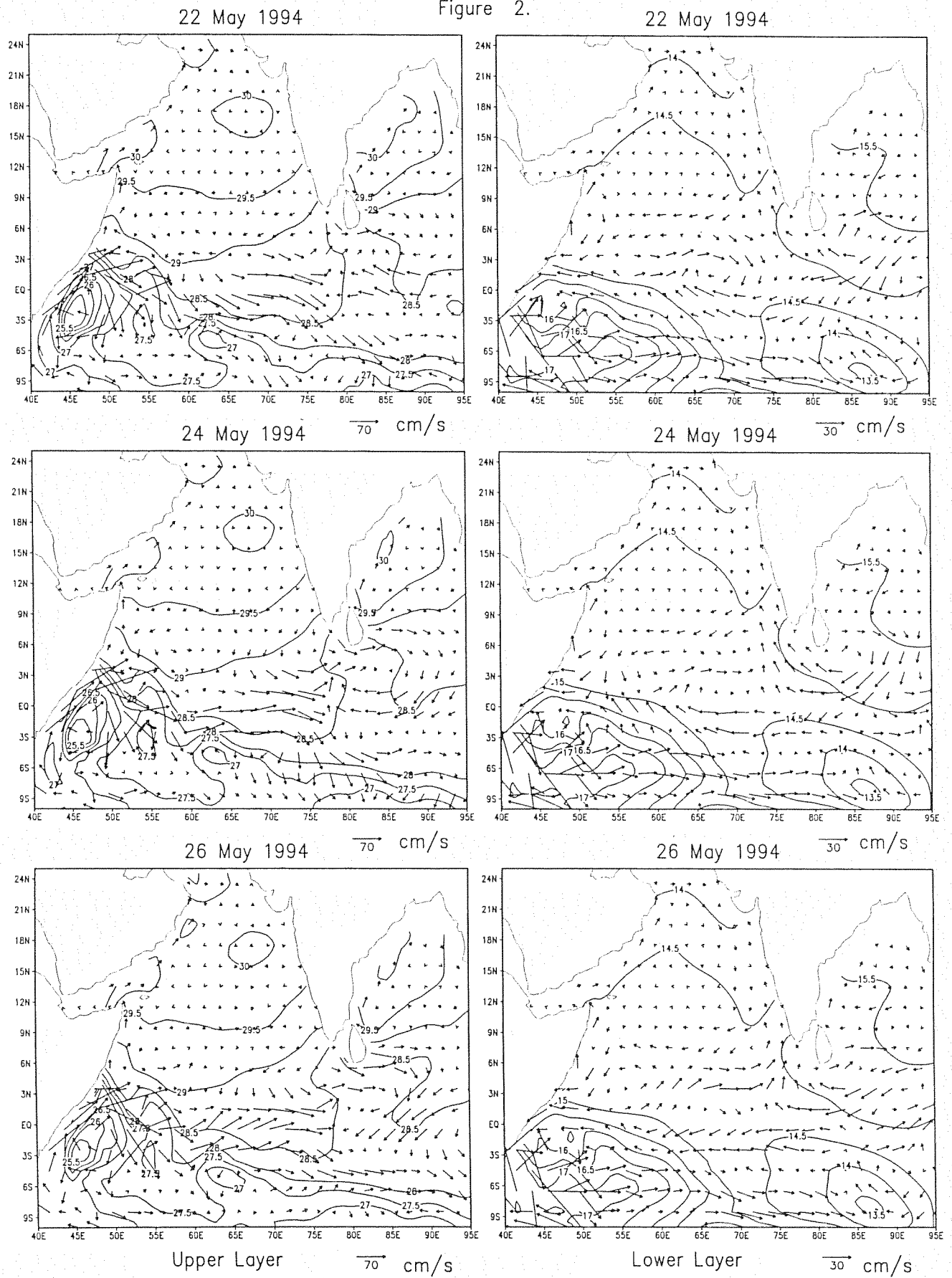


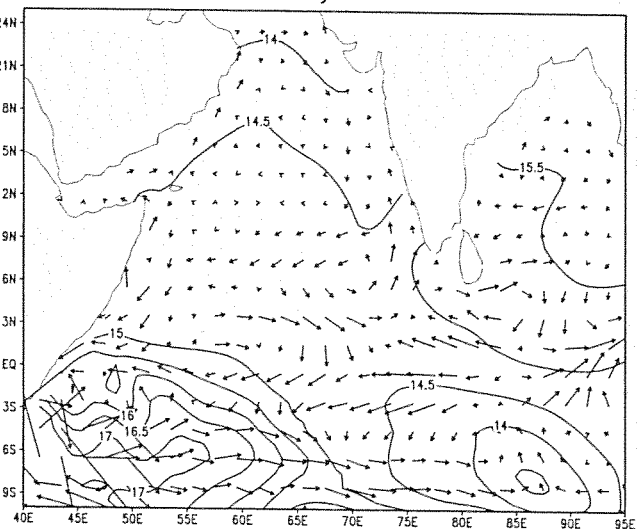
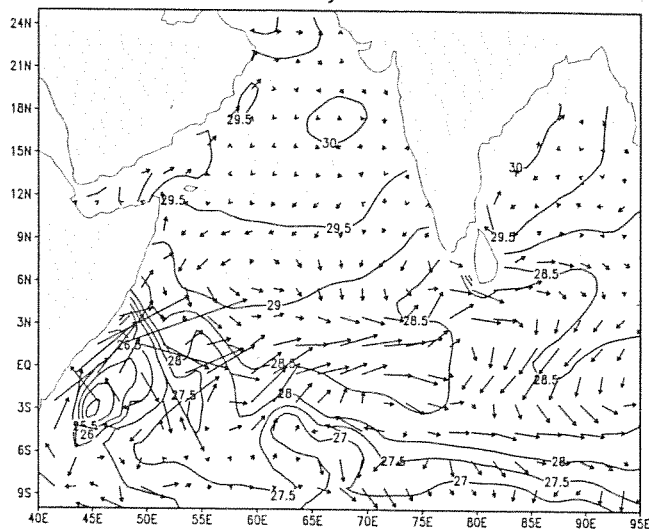
Figure 2.



28 May 1994

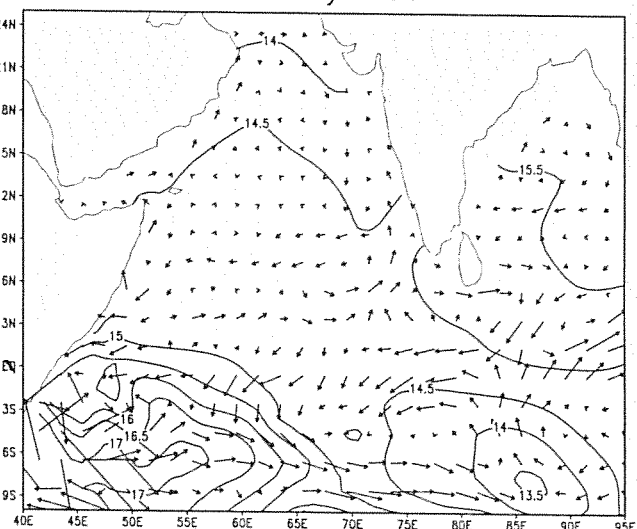
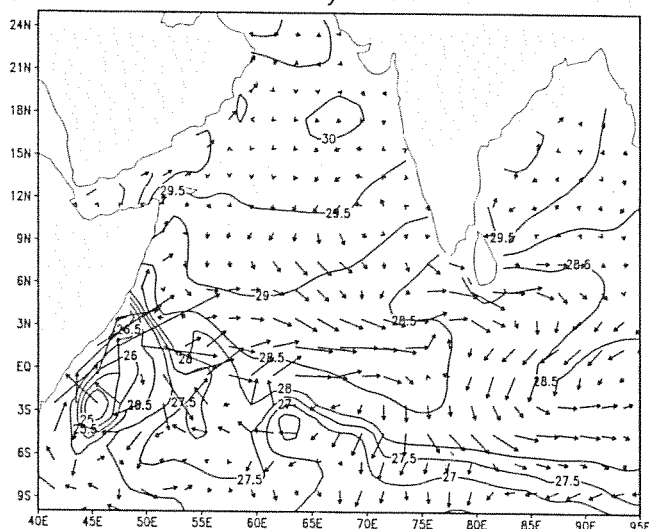
Figure 3.

28 May 1994



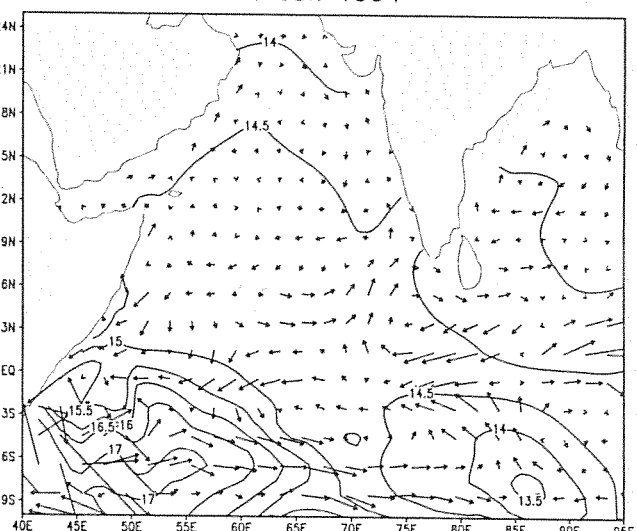
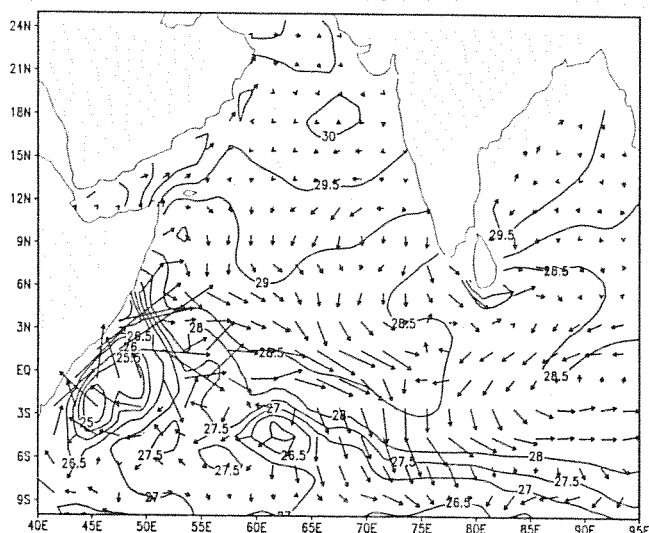
30 May 1994

30 May 1994



1 Jun 1994

1 Jun 1994



Upper Layer

Lower Layer

Figure 4.

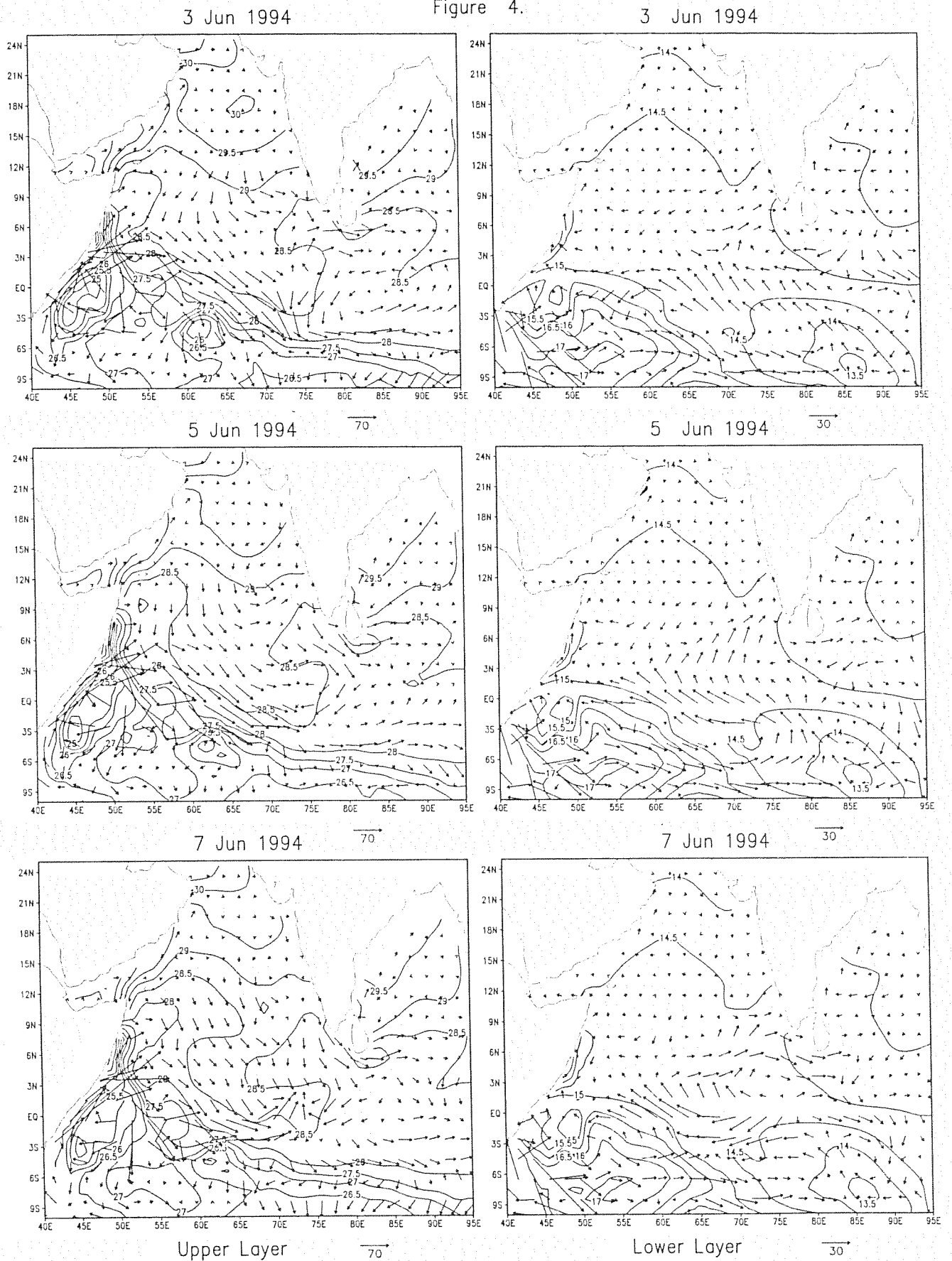


Figure 5.

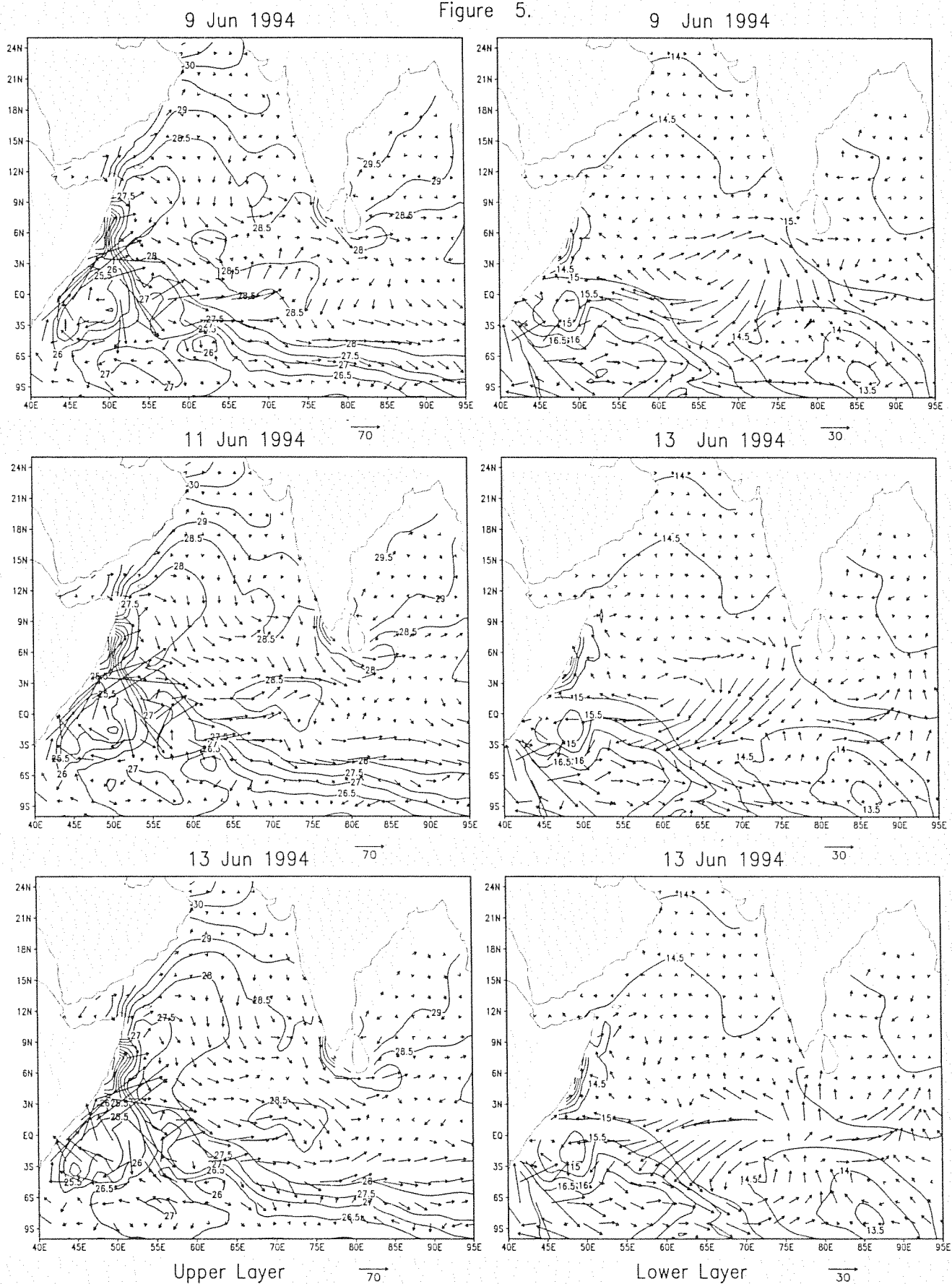


Figure 6.

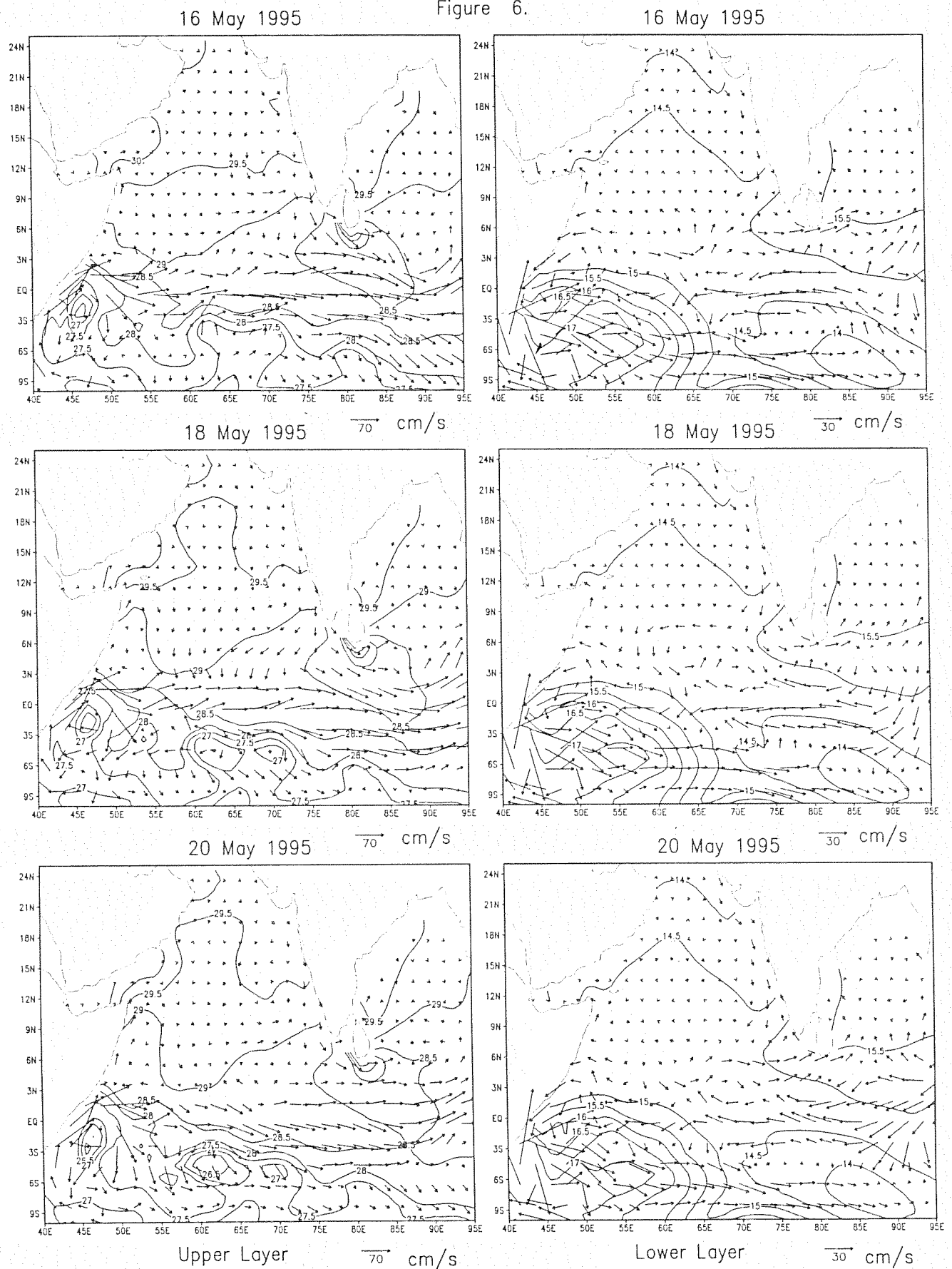


Figure 8.

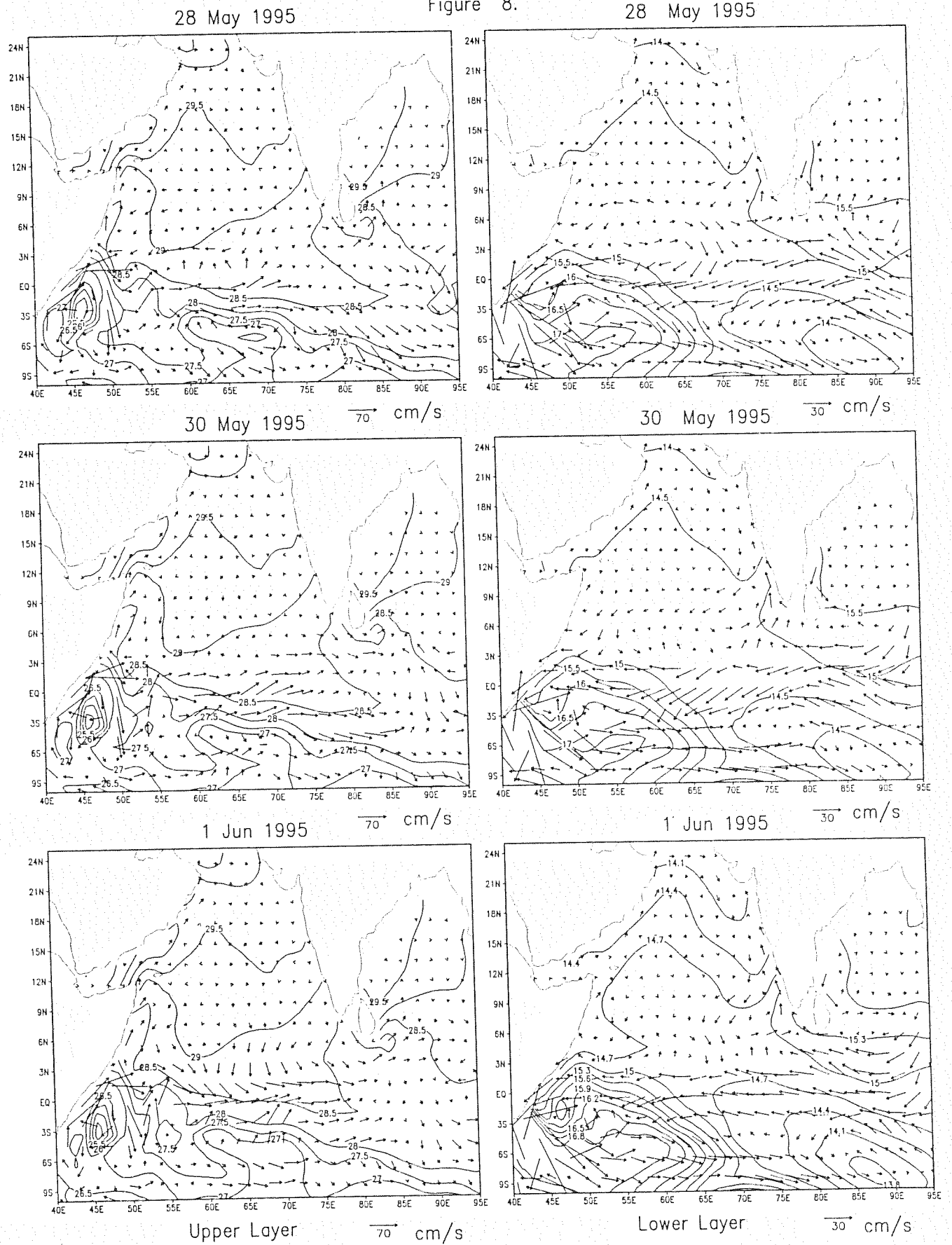


Figure 9.

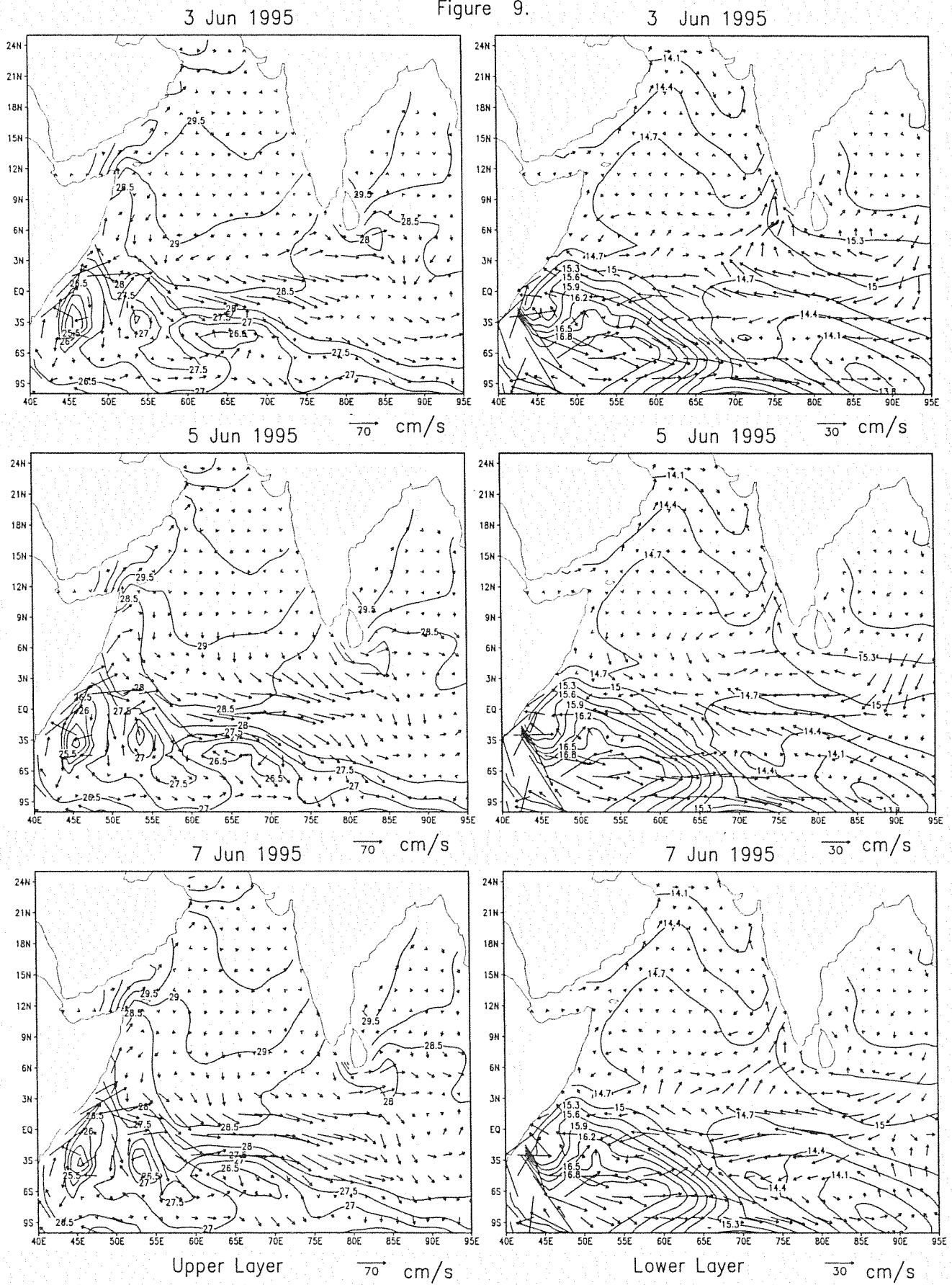


Figure 10.

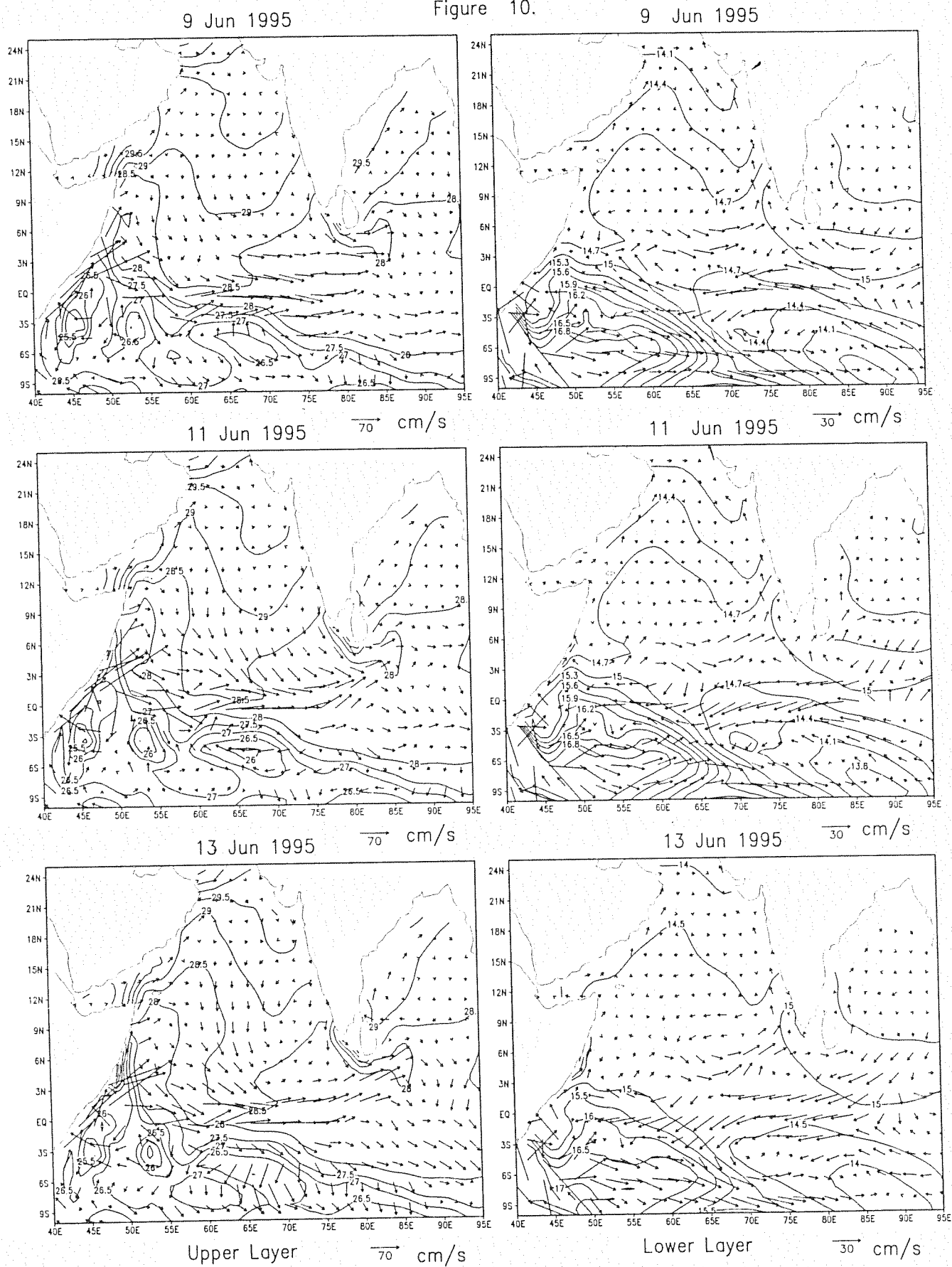


Figure 11.

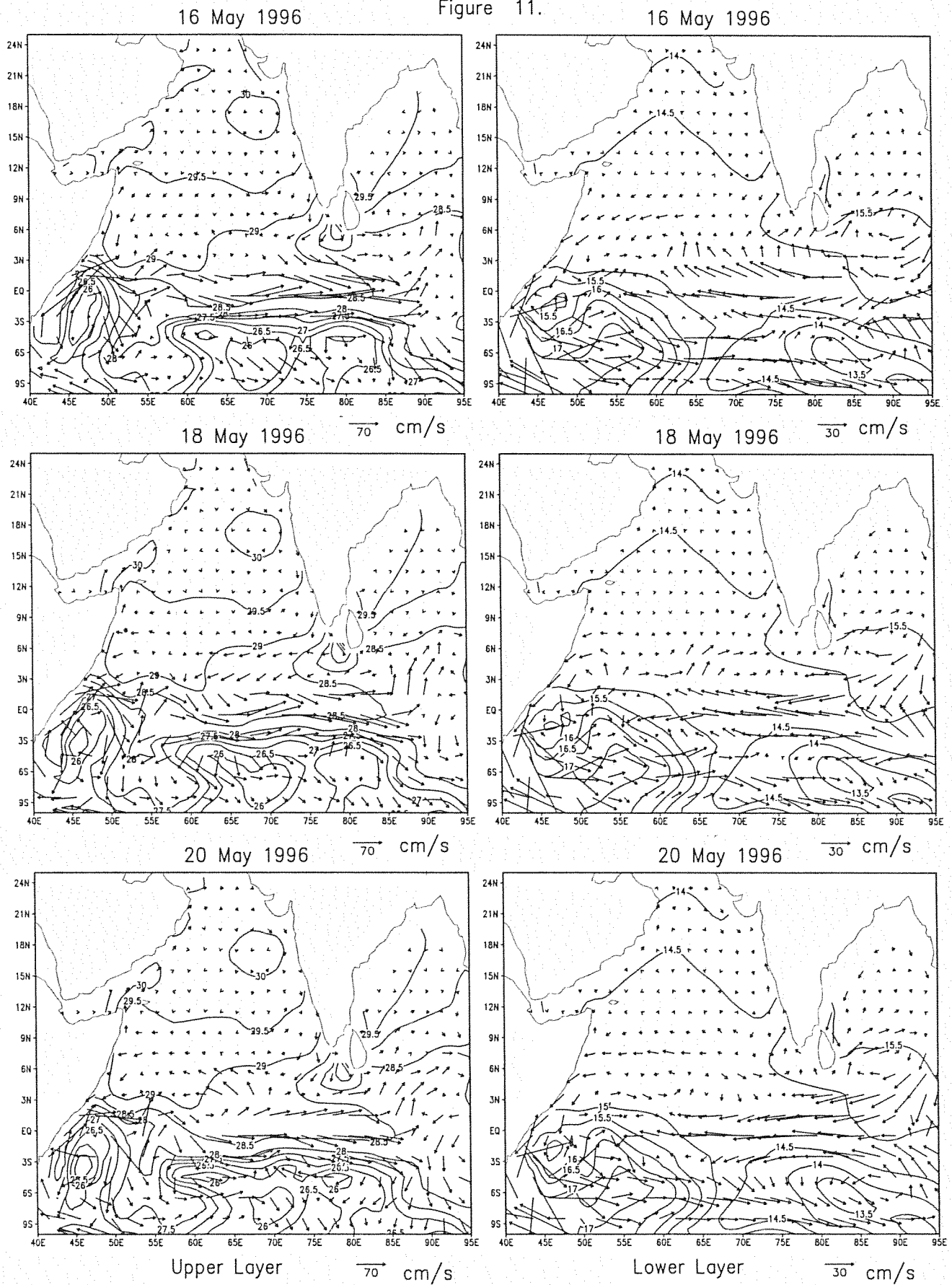


Figure 12.

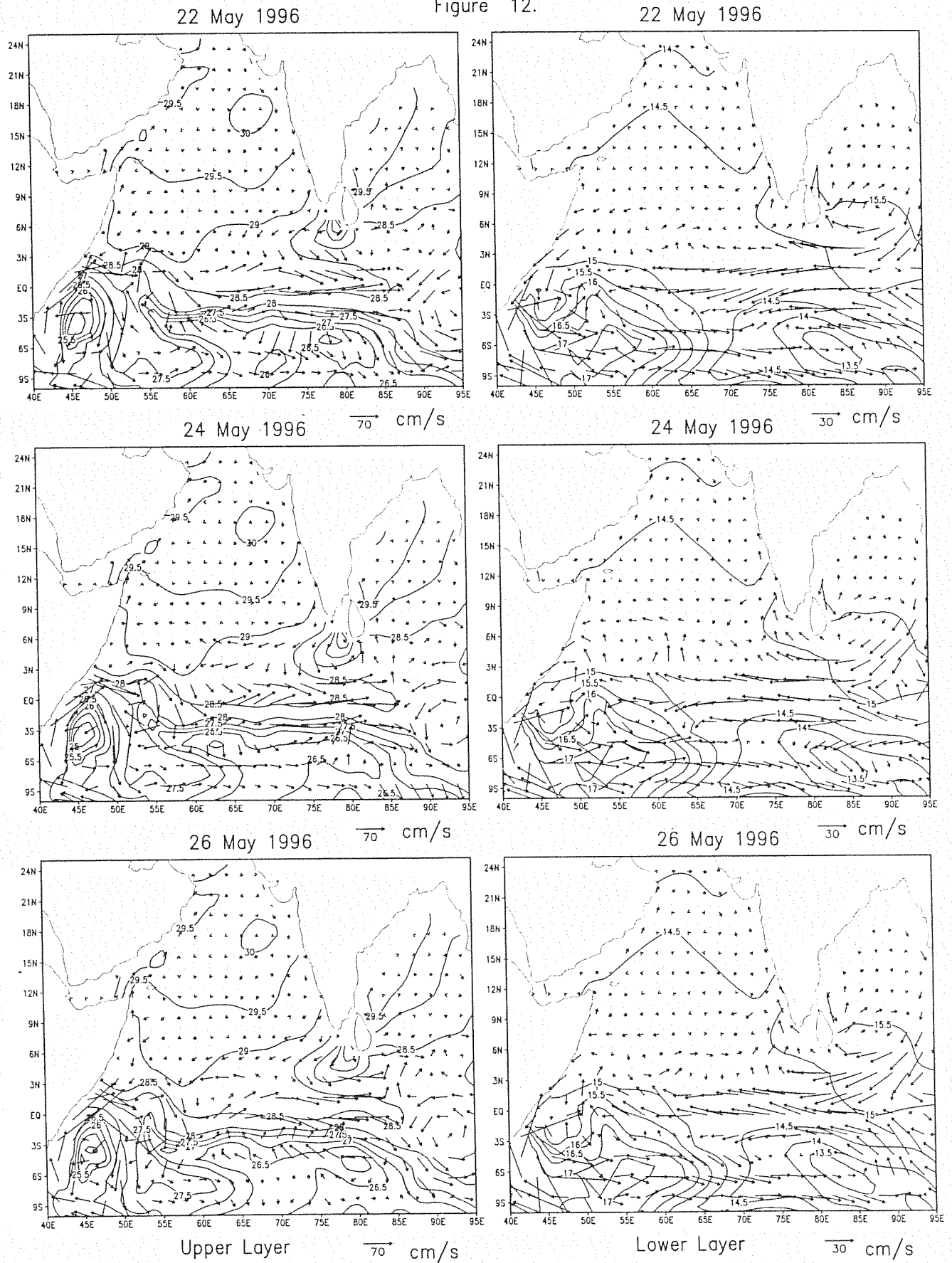


Figure 13.

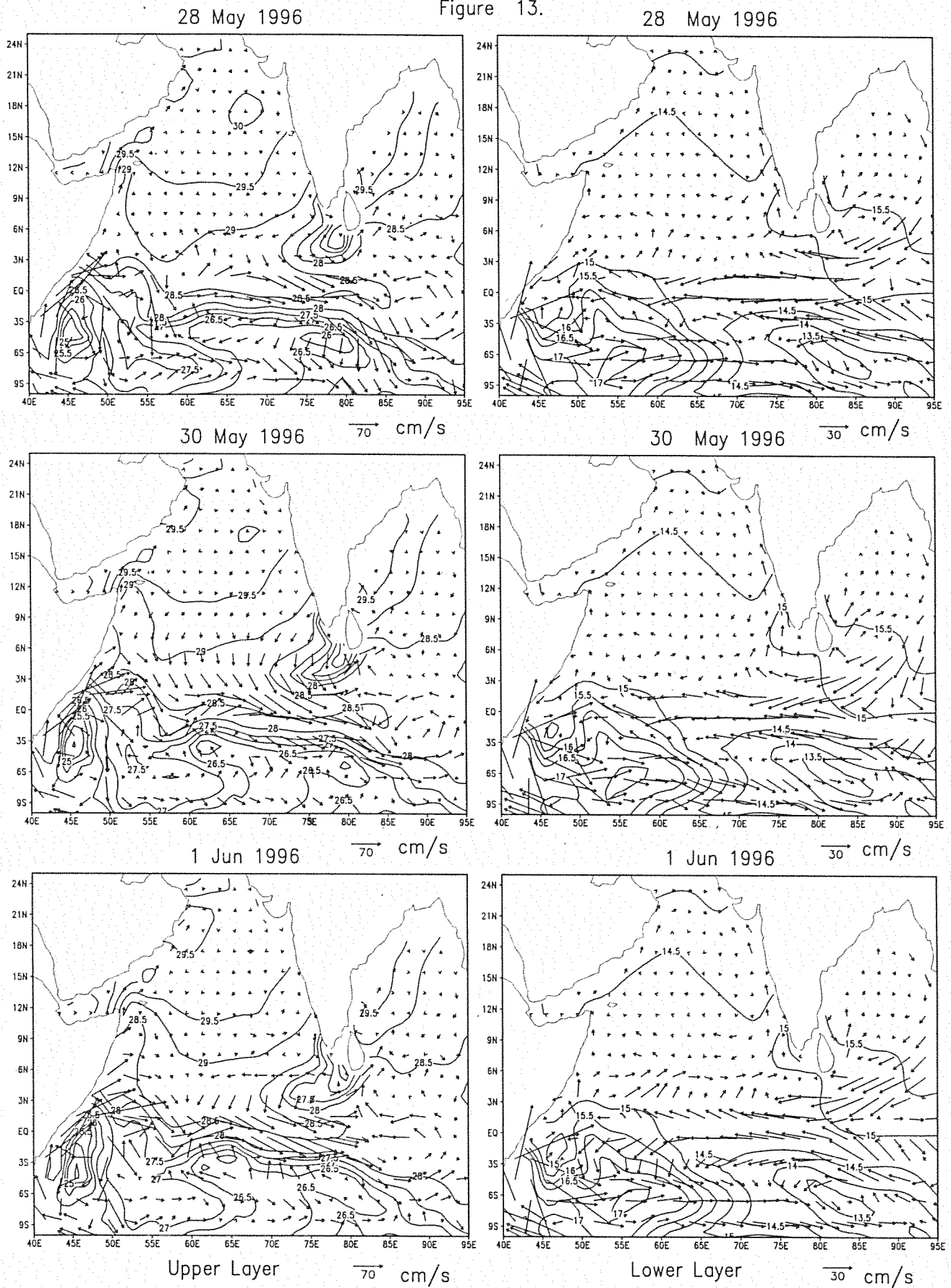


Figure 14.

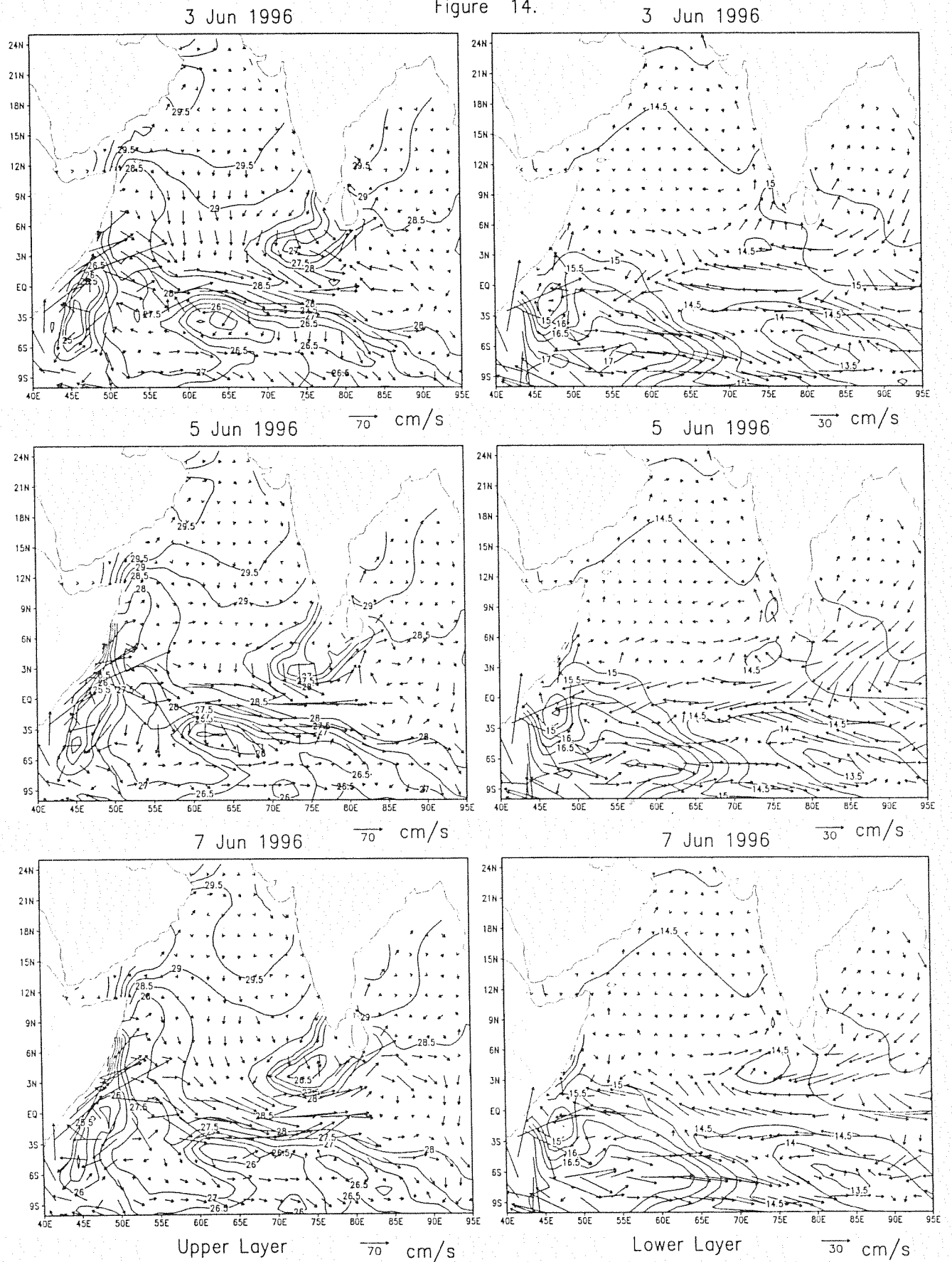


Figure 15.

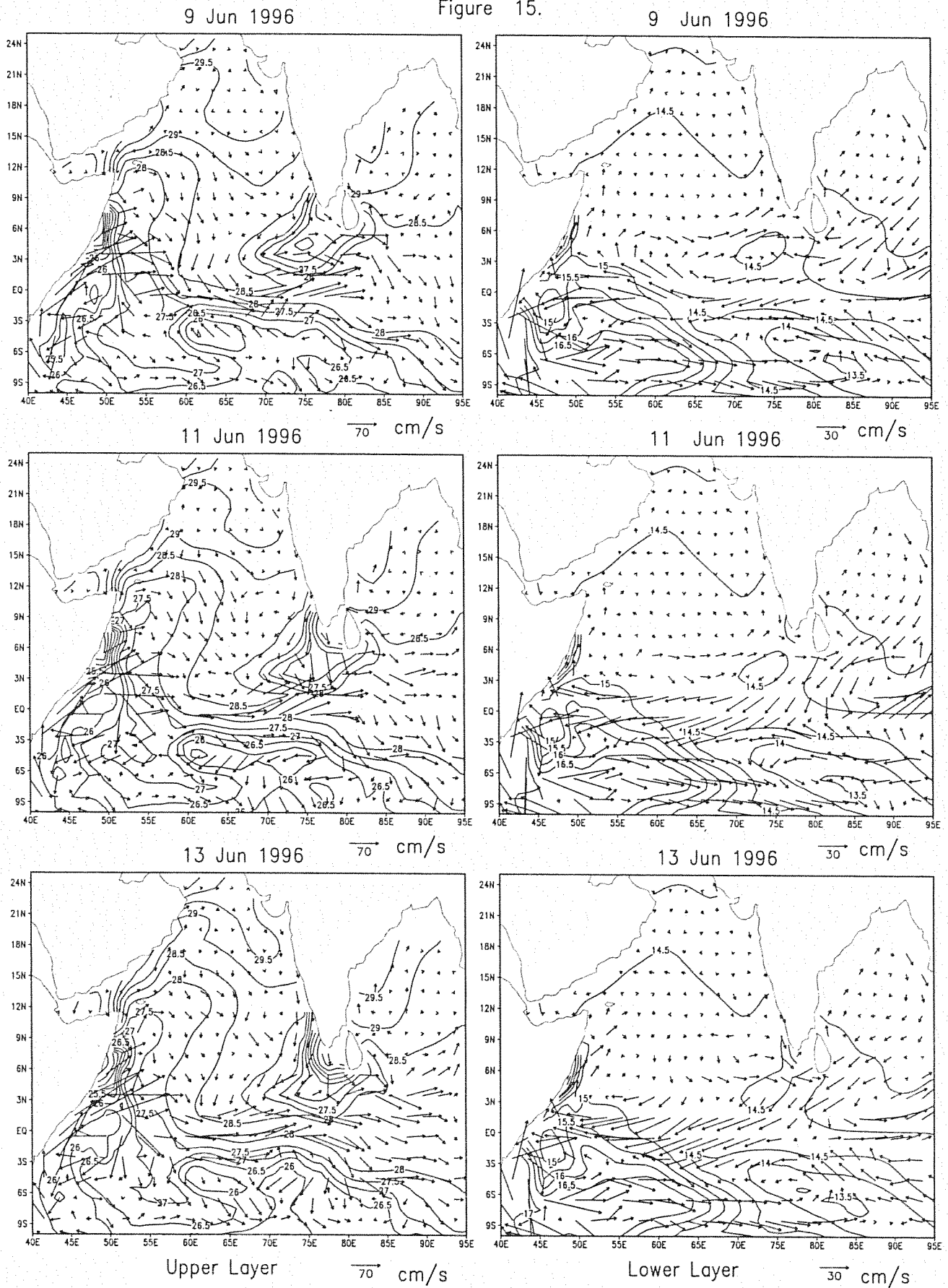


Figure 16.

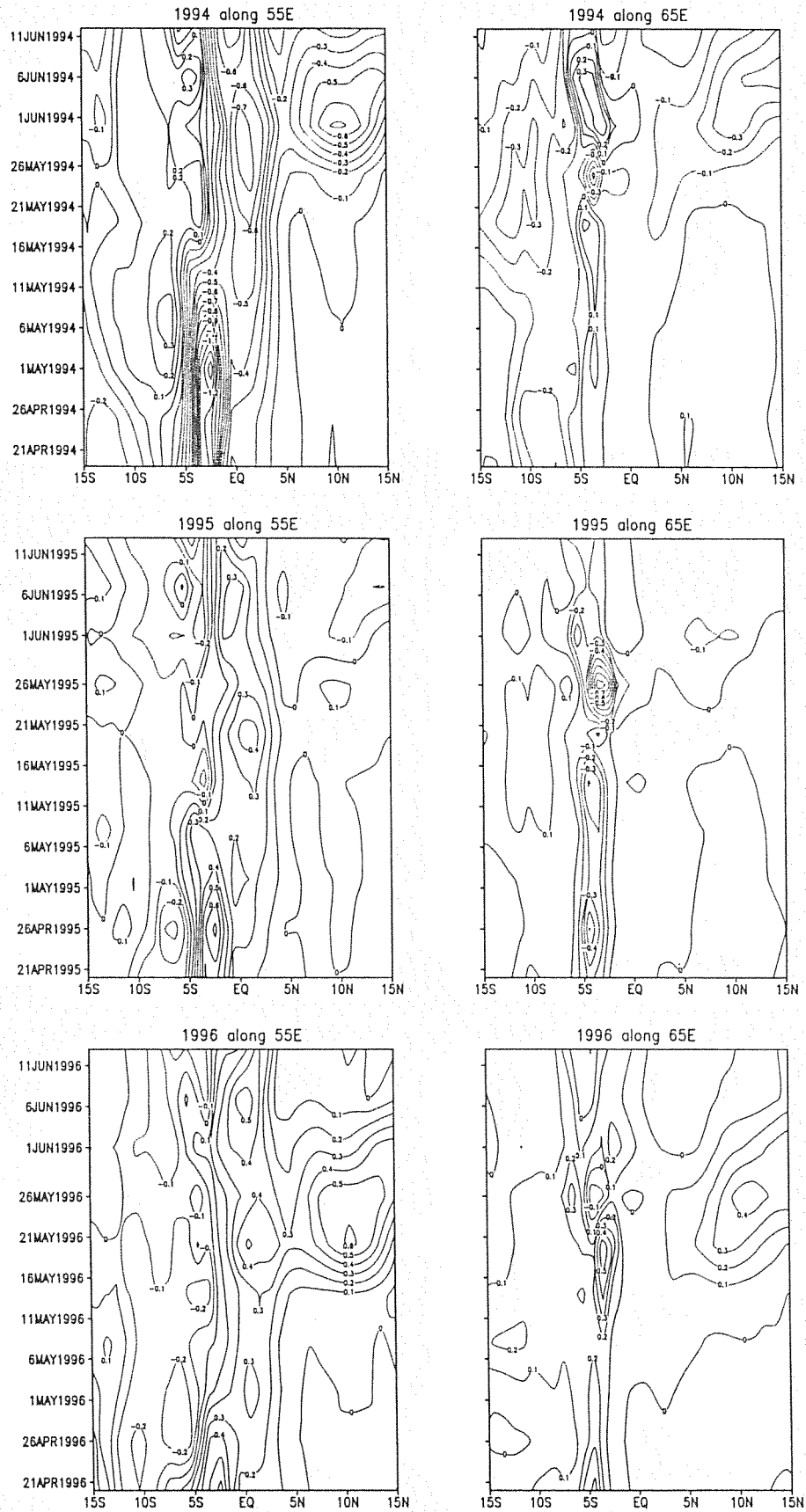
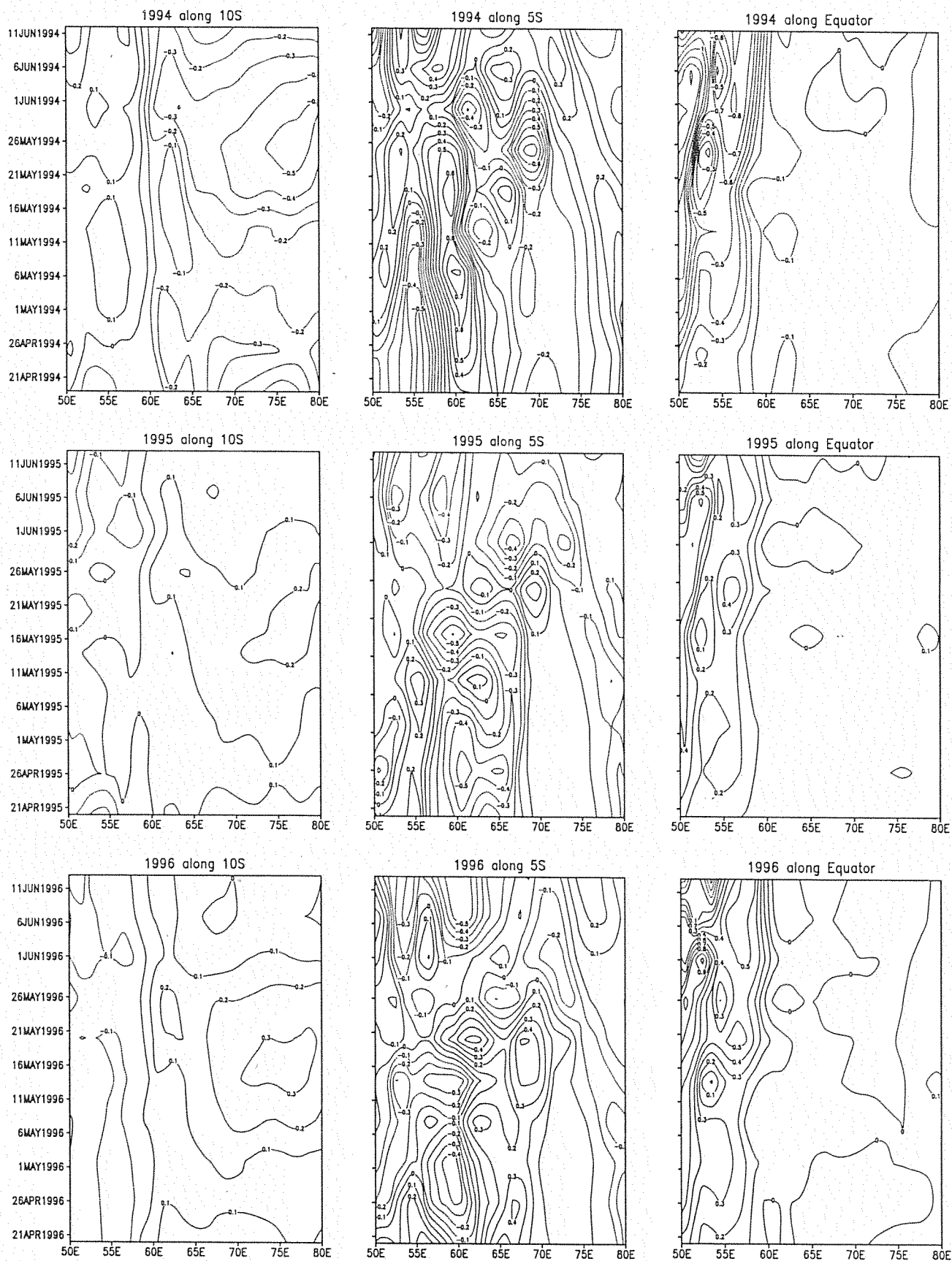


Figure 17.



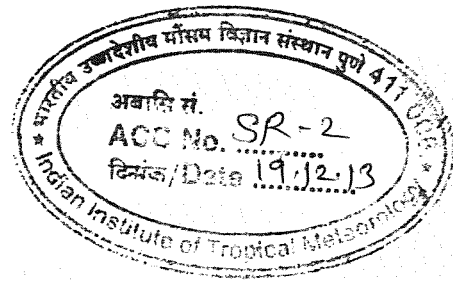


Figure 18.

